MINDO/3 Calculations on Enthalpy and Entropy Effects in the Cyclization of the Hex-5-enyl, 2-Methylhex-5-enyl, and 5-Methylhex-5-enyl Radicals

Enric Canadell *[†]
Department of Chemistry, The University of Chicago, Chicago, Illinois 60637, U.S.A.
Joan Igual
Departament de Química Física, Universitat de Barcelona, Tarragona, Spain

The intramolecular cyclization of the hex-5-enyl radical has been studied by the MINDO/3 method. The effect of methyl substituents in the alkyl and olefin fragments of the radical has been considered. The different electronic and steric effects competing in these reactions have been analysed by means of an energy-partitioning analysis in local contributions. It is shown that the increase in the reaction rate produced by a methyl group in the alkyl part of the radical is due to both enthalpy and entropy effects. The reversal in the regioselectivity from the hex-5-enyl radical to the 5-methylhex-5-enyl radical is due to an enthalpy effect caused by steric and electronic factors.

Free radical addition reactions are in principle very simple chemical processes. However, detailed analysis of both intermolecular and intramolecular additions has given some surprising results. For instance, orientational preferences in intermolecular additions have been shown to be the result of a very subtle balance of several different contributions.[1] A study of regioselectivity in intramolecular radical additions[2] has revealed the inappropriateness of the widely accepted idea in free radical chemistry that radical reactions preferentially afford the most stable radical products.

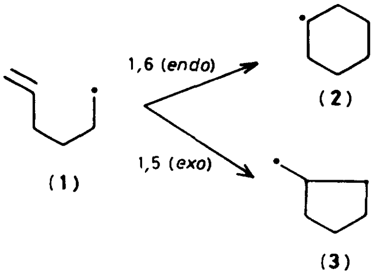

The hex-5-enyl radical (**1**) is one of the main examples of the failure of the thermochemical arguments. There is no ambiguity in the stability of the two possible products of cyclization: the secondary cyclohexyl radical (**2**) is more stable than the primary cyclopentylcarbinyl one (**3**).[3,4] So it is surprising that the cyclization of the hex-5-enyl radical proceeds in a very selective way to afford the cyclopentylcarbinyl radical.[5-7]

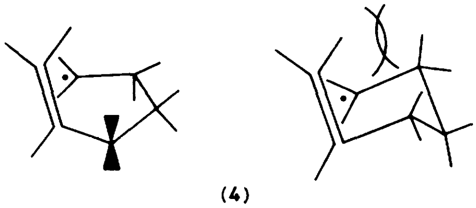

(**4**)

As usually happens when a simple reaction refuses to conform to a widely accepted idea, much work has been devoted to the cyclization of hex-5-enyl radical. Different proposals have been presented to explain the observed regioselectivity. Capon and Rees[8] proposed that a more favourable activation entropy for the formation of the smaller ring was the controlling factor of the regioselectivity. This proposal received some support from both experimental[9] and theoretical[10] work. Nevertheless the difference in activation entropies for 1,5 and 1,6 cyclizations calculated by Bischof,[10] 3.3 cal mol^{-1} K^{-1}, even if in good agreement with experimental estimates by Beckwith and Moad,[7] 2.8 cal mol^{-1} K^{-1}, seems to be insufficient to explain the degree of regioselectivity. Julia and his co-workers[11] proposed that the non-bonded interactions between the *syn* hydrogen at the terminal carbon and the pseudoaxial hydrogen at C-2 were responsible for the destabilization of the 1,6 transition state with respect to that for the 1,5 cyclization (**4**). This interpretation was criticized by Beckwith and Lawrence.[12] Finally, the stereoelectronic requirements of the reaction have been pointed out by Beckwith.[13] The importance of these factors has been nicely demonstrated by the systematic experimental work of Beckwith and his co-workers.[7,14-19] This short survey does not do justice to the extensive experimental work in this area. Some recent reviews give fuller accounts of this work.[2]

We provide here a detailed theoretical discussion of the cyclization of the hex-5-enyl radical and some methyl-substituted derivatives. The structures of the initial and final radicals as well as the transition states have been optimized without any geometrical restriction. This is an imperative requirement in a process in which both enthalpy and entropy effects can be important. Fortunately, earlier work by us[20,21] and others[10,22,23] has shown that the MINDO/3 semiempirical method is probably at its best in the case of hydrocarbon radical additions. Activation energies and kinetic isotope effects were very well reproduced[20,22] for intermolecular additions, showing that both the relative energies of reactants and transition states and the curvature of the potential surface at these points is well accounted for. The results of Bischof[10] and Dewar and Olivella[23] confirm that the method also works very well in intramolecular cases. Even with the use of a semiempirical method the determination of the transition states proved to be an extremely lengthy computational process. The many degrees of freedom and the coupling of different rotational motions lie behind this fact.

There is a second point we would like to stress in this work. When, as it is the case for the systems discussed here, different effects are suggested to explain the experimental results it is often difficult to judge on the relative merits of each one. It is our purpose to show that this problem can be solved by using a partition of the total energy of the transition states and re-

---

[†] *Present address:* Laboratoire de Chimie Théorique, Bât. 490, Université de Paris-Sud, 91405 Orsay, France.

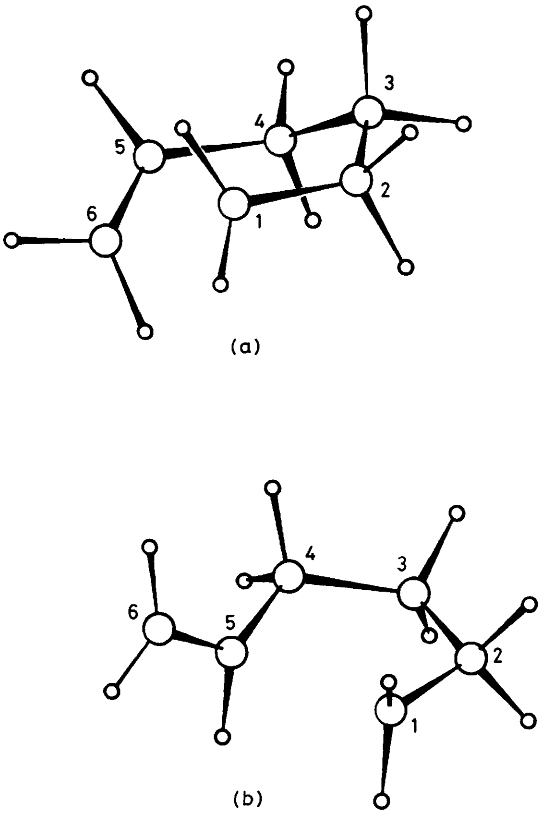

Figure 1. *endo* (a) and *exo* (b) transition states for the cyclization of hex-5-enyl radical

Table 1. Energy-partitioning analysis of the hex-5-enyl radical cyclization. Energies in eV

Energy terms[a]	Initial radical	*exo* TS	*endo* TS	$\Delta_{endo\ \mathrm{TS}-exo\ \mathrm{TS}}$
$E_{\mathrm{C\text{-}1\text{-}C\text{-}5}}$		−1.894		
E^{R}		−2.184		
$E^{\mathrm{N}} + E^{\mathrm{V}} + E^{\mathrm{E}}$		0.290		
$E_{\mathrm{C\text{-}1\text{-}C\text{-}6}}$			−1.436	0.458[b]
E^{R}			−1.717	0.467
$E^{\mathrm{N}} + E^{\mathrm{V}} + E^{\mathrm{E}}$			0.281	0.009
$E_{\mathrm{C\text{-}5\text{-}C\text{-}6}}$	−25.021	−22.755	−23.148	−0.393
E^{R}	−25.818	−24.007	−24.265	−0.258
$E^{\mathrm{N}} + E^{\mathrm{V}} + E^{\mathrm{E}}$	0.798	1.252	1.117	−0.135
$E_{\mathrm{C\text{-}4\text{-}C\text{-}5}}$	−15.893	−15.602	−15.885	−0.283
E^{R}	−17.458	−17.051	−17.418	−0.367
$E^{\mathrm{N}} + E^{\mathrm{V}} + E^{\mathrm{E}}$	1.565	1.449	1.533	0.084
$E_{\mathrm{C\text{-}5}}$	−101.236	−101.632	−101.940	−0.308
E^{U}	−171.874	−171.086	−173.004	−1.918
E^{E}	70.639	69.454	71.064	1.610
$E_{\mathrm{C\text{-}6}}$	−101.750	−102.614	−102.004	0.610
E^{U}	−173.919	−174.498	−172.546	1.952
E^{E}	72.169	71.884	70.542	−1.342
$E_{\mathrm{C\text{-}1}}$	−105.082	−104.758	−104.856	−0.098
E^{U}	−176.799	−175.498	−175.557	−0.059
E^{E}	71.717	70.740	70.701	−0.039

[a] See Figure 1 for notation. [b] Difference between the $E_{\mathrm{C\text{-}1\text{-}C\text{-}6}}$ (*endo* TS) and the $E_{\mathrm{C\text{-}1\text{-}C\text{-}5}}$ (*exo* TS).

actants in mono- and bi-centric local contributions.[24] In this way we can dissect the total energy in contributions associated with atoms, bonds, and non-bonded pairs and, consequently, the strength of the different effects can be evaluated.

Theoretical Procedure

The calculations were carried out by using the spin-unrestricted version of MINDO/3 with standard parameters.[25] Although the use of an unrestricted wavefunction suffers from the theoretical objection that it is not an eigenfunction of the total spin angular momentum operator S^2, this problem did not raise any difficulty in the present calculations because the calculated values of S^2 indicated that the contamination by higher spin states was unimportant.

All equilibrium geometries were determined by minimizing the total energy with respect to all geometrical parameters using the standard Davidon–Fletcher–Powell procedure.[26] The transition states were found by the usual reaction co-ordinate method and refined by minimizing the scalar gradient of the energy.[27] All stationary points were checked by calculating and diagonalizing the Hessian (force constant) matrix by using cartesian co-ordinates. Convergence was confirmed by the presence of six near-zero eigenvalues, all other eigenvalues being positive for minima but one negative for transition states.[27]

Molecular entropies were obtained from the calculated geometries and vibrational frequencies in the usual manner.[28]

Results and Discussion

Cyclization of the Hex-5-enyl Radical.—The MINDO/3 transition states for the 1,5 and 1,6 cyclizations were reported by Bischof.[10] Lee has briefly commented on these results.[29] Let us discuss at some length the electronic changes during this reaction. There are several reasons for discussing this process again. First, Bischof reported the transition-state structures without much comment on the electronic changes. Second, it is obviously the reference point for discussing substituent effects. Third, it is the simplest way to illustrate the use of energy partitioning.

The two transition states are shown in Figure 1. As reported previously[10] the activation enthalpy is 16.5 kcal mol^{-1}. The enthalpy difference between the two transition states is almost nil but the activation entropy favours *exo* cyclization by 3.6 cal mol^{-1} K^{-1}. The small discrepancy with Bischof's result with respect to the activation entropies is due to the fact that because of the more restrictive criteria used in the transition-state search we were able to calculate the entropies directly from the vibrational frequencies and not in an approximate way as previously done.[10] The calculated heats of reaction are −16.3 and −34.3 kcal mol^{-1} for *exo* and *endo* cyclizations respectively. of the more restrictive criteria used in the transition-state (2.200 *versus* 2.265 Å). These bond lengths are shorter than those found in intermolecular additions.[20–22] There is only a very small change in the olefinic bond [1.357 Å in (**3**) and 1.352 Å in (**2**)] with respect to the initial radical (1.327 Å) as found in the intermolecular reactions. Because there are only minor differences the reader is directed to the work of Bischof[10] for further structural details.

Let us proceed to the energy-partitioning analysis. The main mono- and bi-centric contributions are collected in Table 1. The terms not shown there do not differentiate between the two structures. The total bicentric terms can be partitioned in a resonance term ($E^{\mathrm{R}}_{\mathrm{AB}}$), which represents the non-classical energy stabilization due to delocalization, and an electrostatic contribution ($E^{\mathrm{N}}_{\mathrm{AB}} + E^{\mathrm{E}}_{\mathrm{AB}} + E^{\mathrm{V}}_{\mathrm{AB}}$), which contains the

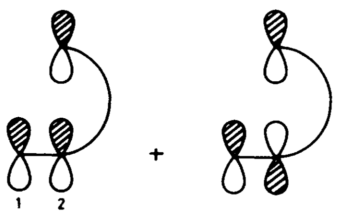

(5)

repulsive core–core (E^{N}_{AB}) and electron–electron (E^{E}_{AB}) terms and the attractive electron–core (E^{V}_{AB}) one. The monocentric terms contain an attractive core–electron part (E^{U}_{A}) and a repulsive electron–electron one (E^{A}_{AB}). Despite the fact that the olefinic distance (C-5–C-6) is the same in both transition states, the corresponding energy term shows a strong difference, the *endo* transition states being favoured. A very important destabilization with respect to the initial radical should be noticed. The newly created bond conforms more closely to the geometric picture: the more stabilizing term corresponds to the shorter bond. Interestingly, the electrostatic contribution is almost exactly the same in both cases. So, notwithstanding the geometrical data, the olefinic bond is more broken and the newly formed bond more strong in the *exo* transition state.

How can we understand these results? The main electronic event in a radical addition is the transfer of the unpaired electron from the incoming radical centre to the non-attacked olefinic carbon. In the first stage of the reaction, this transfer is accomplished by the mixing of the α odd electron orbital with the HOMO (α) and the LUMO (α) of the local olefinic part. Because this is a three-orbital interaction the radical orbital mixes in π and π^* with opposite signs as in (5). The coefficient at C-2 decreases and that at C-1 increases. As a result there is an accumulation of α electron density at C-1. In a UHF treatment this is supplemented by an electronic shift of the β electron density in the opposite direction. It is only when there is enough β electron density at C-2 that the new bond is established. We then identify the spin polarization of the olefin as the main source of electronic energy barrier in these reactions.

This simple interpretation is fully supported by the results of Table 1. The *exo* transition state which has the more formed new bond has also the more broken (in an electronic sense) olefinic bond as evidenced by the $E_{C\text{-}5\text{–}C\text{-}6}$ energy term and by the spin-population analysis of the transition states (Table 2). The *exo* transition state presents the largest spin polarization. Other results of Table 1 are worthy of comment. The $E_{C\text{-}4\text{–}C\text{-}5}$ term which corresponds to the bond adjacent to the olefinic part clearly favours the *endo* transition state. Again this result is due to the resonance contribution. When this term is compared with the value in the initial radical, it is clearly seen that the bond is destabilized in the *exo* transition state while it remains unaltered in the *endo*. This is the result of a shift of β electron density towards the attacked carbon in the *exo* transition state in order to facilitate bond formation. This effect cannot occur in the *endo* transition state.

It is pertinent at this point to recall some results from our analysis of the regioselectivity in intermolecular addition.[21] Contrary to some early proposals[30] we showed that the SOMO–HOMO component of the three-orbital interaction (5) is much more important than the SOMO–LUMO one and thus controls the regioselectivity of the reaction. As this interaction is stabilizing* the attack is produced at the carbon atom with the greater coefficient in the HOMO of the olefin. Due to the well known polarization effect of the alkyl groups[31] the attack is produced at the less substituted carbon. The analysis of the evolution of the molecular orbitals in the present case shows that essentially the same type of interactions are operative. This seems to be in contradiction with the energy results. In fact there is an important difference between the inter- and intramolecular cases. While in the former case the radical is free to find the most efficient SOMO–HOMO overlap, in the latter the cyclic nature of the process can considerably restrict this freedom. Close examination of the transition states shows that in the *exo* transition state the orbitals of the two interacting carbons are better orientated to overlap and this fact counterbalances the effect of the initial polarization of the double bond which favours the *endo* transition state.

A final remark has to be made on the energy cost of olefin polarization. The polarization of the bond results in a destabilization of the bicentric term but a secondary effect of this electron redistribution is that the monocentric terms are stabilized. Although the changes on the monocentric terms $E_{C\text{-}5}$ and $E_{C\text{-}6}$ cannot be considered to come exclusively from olefin polarization (recall the electronic shift through the adjacent C-5–C-4 bond), the values in Table 1 clearly show that the polarization required before the interactions leading to the formation of the new bond begin to dominate the process is not an energetically very costly process.

Before considering how this analysis is modified by the presence of substituents let us comment on the above mentioned proposal of Julia.[11] The term corresponding to the non-bonded hydrogen atoms in the *endo* transition state [see (4)] is almost nil (0.001 eV). The repulsive electron–electron and core–core terms are by no means negligible but they are exactly balanced by the attractive electron–core term. This result strongly argues against this interpretation and substantiates the results of Beckwith and Lawrence.[12] These authors showed that when the two hydrogens were substituted by methyl groups the transition state was destabilized by only 0.8 kcal mol^{-1}.

The origin of the differential entropy effect will be discussed later. Finally, we point out that the MINDO/3 method underestimates the strain energy in cyclohexane.[32] Although on a lesser extent this fact also affects the 1,6 transition state. In consequence, a small enthalpy contribution probably also favours 1,6 cyclization. As the effect of this incipient strain energy is small and spread out over all the ring, the above analysis will be almost unaffected.

Cyclization of the 5-Methylhex-5-enyl Radical. Effect of a Methyl Group in the Olefinic Fragment of the Radical.—The introduction of a methyl group at the 5-position in the hex-5-enyl radical has a strong effect on the regioselectivity of the cyclization. The *endo* mode is now preferred over the *exo*.[12,33] The thermochemical explanation would predict an increase in $k_{1,6}$ and a small change in $k_{1,5}$ with respect to the unsubstituted radical. However, the experimental results show that the reversal in the regioselectivity is due to a small increase in $k_{1,6}$ and a strong decrease in $k_{1,5}$. The MINDO/3 transition states for the two cyclization modes are shown in Figure 2 and the main structural parameters of the reactant, products, and transition states are reported in Table 3.

The activation enthalpies for the 1,5 and 1,6 cyclizations are 22.3 and 14.6 kcal mol^{-1}, respectively, while the corresponding value for the unsubstituted radical is 16.5 kcal mol^{-1}. The differences seem to be somewhat exaggerated but the trend is in excellent agreement with the experimental results.[12,33] The activation entropy favours 1,5 cyclization by 3.8 cal mol^{-1} K^{-1}, also in good agreement with the experimental value. The heats of reaction are -3.2 and -39.4 kcal mol^{-1} for *exo* and *endo* cyclization, respectively.

---

* A three-electron two-orbital interaction can be either stabilizing or destabilizing when overlap is taken into account. Because of the long C ⋯ C distances in the transition states the interaction is stabilizing in the addition reactions.[21]

Table 2. Electron and spin densities for the initial radical and transition states of the cyclizations of the hex-5-enyl, 2-methylhex-5-enyl, and 5-methylhex-5-enyl radicals

	Electron density			Spin density		
	Initial radical	*exo* TS	*endo* TS	Initial radical	*exo* TS	*endo* TS
			Hex-5-enyl radical			
C-1	4.090	4.047	4.048	1.118	0.935	0.951
C-5	4.032	3.966	4.013	0.000	−0.437	0.469
C-6	3.990	4.043	3.994	0.000	0.582	−0.392
			5-Methylhex-5-enyl radical			
C-1	4.090	4.047	4.048	1.119	0.891	0.961
C-5	3.988	3.954	4.006	0.000	−0.503	0.462
C-6	4.036	4.056	4.010	0.000	0.716	−0.450
			2-Methylhex-5-enyl radical			
C-1	4.097	4.050	4.051	1.126	0.941	0.955
C-5	3.989	3.986	4.014	0.000	−0.430	0.471
C-6	4.032	4.041	3.992	0.000	0.570	−0.391

Table 3. Calculated geometries for the reactant, products, and transition states of the cyclization of 5-methylhex-5-enyl radical

	Geometry[a,b]
5-Methylhex-5-enyl radical	C-1C-2: 1.455; C-2C-3: 1.514; C-3C-4: 1.517; C-4C-5: 1.517; C-5C-6: 1.344; C-5C-7: 1.497; C-1C-2C-3: 120.6; C-2C-3C-4: 119.8; C-3C-4C-5: 120.2; C-4C-5C-6: 121.7; C-7C-5C-6: 120.7; C-1C-2C-3C-4: 179.0; C-2C-3C-4C-5: 184.1; C-3C-4C-5C-6: 120.2; HC-1C-2C-3: −26.3; H′C-1C-2C-3: 169.1; C-7C-5C-6C-4: 178.1
1-Methylcyclohexyl radical	C-1C-2: 1.518; C-2C-3: 1.519; C-3C-4: 1.519; C-4C-5: 1.502; C-5C-6: 1.503; C-6C-1: 1.519; C-5C-7: 1.479; C-5C-6C-1: 118.9; C-6C-1C-2: 116.6; C-1C-2C-3: 116.1; C-2C-3C-4: 117.1; C-3C-4C-5: 118.9; C-4C-5C-6: 119.0; C-7C-5C-6: 120.5; C-4C-3C-2C-1: 35.8; C-5C-4C-3C-2: −26.3; C-6C-1C-2C-3: −37.2
(1-Methylcyclopentyl)methyl radical	C-1C-2: 1.520; C-2C-3: 1.520; C-3C-4: 1.523; C-4C-5: 1.570; C-5C-6: 1.493; C-5C-1: 1.570; C-5C-7: 1.535; C-6C-5C-7: 107.5; C-6C-5C-1: 112.0; C-5C-1C-2: 110.0; C-4C-5C-1: 103.0; C-3C-4C-5: 110.5; HC-6C-5H′: 159.0; C-5C-1C-2C-3: 7.3; C-4C-3C-2C-1: 2.8; HC-7C-5C-4: 62.0
exo TS	C-1C-2: 1.480; C-2C-3: 1.518; C-3C-4: 1.520; C-4C-5: 1.532: C-5C-6: 1.387; C-5C-7: 1.506; C-1C-5: 2.170; C-1C-5C-6: 99.0; C-2C-3C-4: 114.7; C-3C-4C-5: 117.1; C-6C-5C-4: 119.7; C-7C-5C-6: 117.7; HC-1C-2: 104.1; H′C-1C-2: 106.0; C-1C-5C-6C-4: −99.1; C-2C-3C-4C-5: −9.0; C-3C-4C-5C-6: −98.3; C-4C-6C-5C-7: 151.8; HC-1C-5C-6: 114.9; H′C-1C-5C-6: −1.1; HC-6C-5C-4: 17.5; H′C-6C-5C-4: −171.5
endo TS	C-1C-2: 1.475; C-2C-3: 1.519; C-3C-4: 1.522; C-4C-5: 1.516; C-5C-6: 1.370; C-5C-7: 1.491; C-1C-6: 2.300; C-1C-2C-3: 119.1; C-2C-3C-4: 119.6; C-3C-4C-5: 116.6; C-6C-1C-2: 106.2; HC-6C-5: 123.4; H′C-6C-5: 124.7; HC-1C-2: 118.4; H′C-1C-2: 118.4; C-1C-2C-3C-4: 40.3; C-2C-3C-4C-5: 44.7; C-6C-1C-2C-3: −36.6; C-7C-5C-4C-3: −106.8; C-4C-5C-6H: −175.4; C-4C-5C-6H′: 25.6; HC-1C-2C-3: −149.9; H′C-1C-2C-3: 73.9

[a] Distance in Ångstroms, angles in degrees. [b] See Figure 2 for notation.

Table 4. Energy-partitioning analysis of the cyclization of 5-methylhex-5-enyl radical. Energies in eV

Energy terms[a]	Initial radical	*exo* TS	*endo* TS	$\Delta_{endo\ TS - exo\ TS}$
$E_{C\text{-}1\text{–}C\text{-}5}$		−2.390		
$E_{C\text{-}1\text{–}C\text{-}6}$			−1.330	1.060[b]
$E_{C\text{-}5\text{–}C\text{-}6}$	−24.392	−21.261	−22.435	−1.174
$E_{C\text{-}4\text{–}C\text{-}5}$	−15.306	−14.977	−15.334	−0.357
$E_{C\text{-}5\text{–}C\text{-}7}$	−15.777	−15.556	−15.941	−0.385
$E_{C\text{-}1\text{–}CH_3}$		0.183	0.000	−0.183
$E_{C\text{-}1}$	−105.087	−104.656	−104.860	−0.204
$E_{C\text{-}5}$	−100.986	−101.547	−101.660	−0.113
$E_{C\text{-}6}$	−101.886	−103.164	−102.266	0.898
$E_{C\text{-}7}$	−101.040	−101.110	−100.991	0.119

[a] See Figure 2 for notation. [b] Difference between the $E_{C\text{-}1\text{–}C\text{-}6}$ (*endo*) and the $E_{C\text{-}1\text{–}C\text{-}5}$ (*exo*).

The newly formed bond is shorter in the 1,5 transition state (2.170 *versus* 2.300 Å) while the olefinic bond is shorter in the 1,6 (1.370 *versus* 1.387 Å). The comparison with the olefinic distance in the initial radical (1.344 Å) shows that the lengthening of this bond is again rather small in both transition states. Taking as reaction co-ordinate the new $C \cdots C$ bond distance we can conclude that the introduction of the methyl results in an earlier 1,6 and a later 1,5 transition state. As Beckwith has pointed out[2a] a purely steric explanation of the regioselectivity change is not likely. We can analyse this point by using the energy-partitioning analysis (Table 4). Only the total values for the different terms have been included in Table 4. As found before (Table 1) the main component of the bicentric terms is the resonance one with the only exception of the non-bonded C-1–CH_3 term where the electrostatic terms are the only important ones. The new bond is more formed in the *exo*

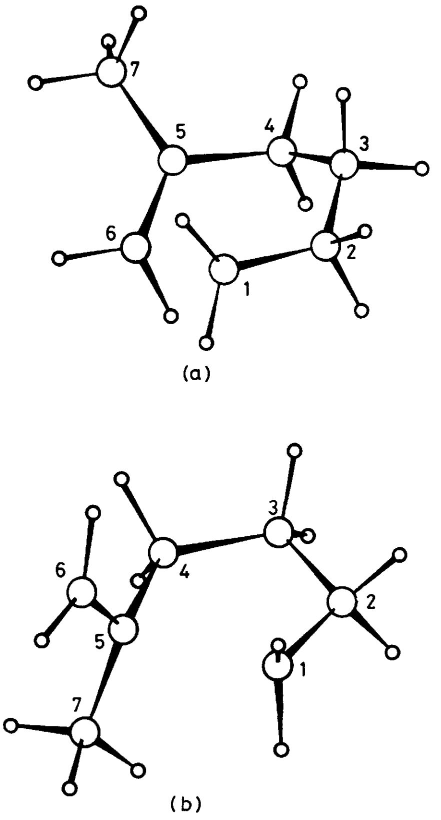

Figure 2. *endo* (a) and *exo* (b) transition states for the cyclization of 5-methylhex-5-enyl radical

transition state and the olefinic bond is less broken in the *endo*. Again this last result contrasts with the small difference in the corresponding bond lengths. As can be seen from Table 2 the spin polarization in the *exo* transition state is larger than in the *endo* and also larger than in the *exo* transition state of the unsubstituted radical. Comparison of the $E_{C\text{-}5\text{--}C\text{-}6}$ term with the values in the initial and final radicals shows that the olefinic bond is one-third broken in the *exo* transition state but one-fourth in the *endo*. The globial contribution of the new bond and the olefinic one favour the *endo* route.

The $E_{C\text{-}4\text{--}C\text{-}5}$ and $E_{C\text{-}5\text{--}C\text{-}7}$ contributions both favour the *endo* transition state. The analysis of the first one is completely equivalent to that presented for the unsubstituted case and will not be repeated here. The $E_{C\text{-}5\text{--}C\text{-}7}$ term, which corresponds to the bond with the substituent, shows that this bond has been stabilized in the *endo* transition state but destabilized in the *exo*. In the *exo* transition state the substituent is bonded to the atom being attacked and so there is a shift of β electron density towards this carbon which facilitates the reaction. The situation is the same as for the C-4–C-5 bond. In contrast, in the *endo* transition state the substituent is bonded to the atom where the α electron density accumulates. In order to prevent excessive electron–electron repulsions (which will affect the monocentric term) part of this electron density is delocalized towards the substituent reinforcing the bond. In fact, this delocalization is the same which makes the tertiary radicals more stable than the secondary ones. The influence of the stability of the final radical appears in the energy-partitioning analysis through this term. It is this effect which is in the main responsible for the increase of $k_{1,6}$. The non-bonded repulsions due to the substituent ($E_{C\text{-}1\text{--}CH_3}$) contribute 0.183 eV to the destabilization of the *exo* with respect to the *endo* transition state. When comparing the activation enthalpies for the unsubstituted and substituted radicals, *exo* cyclization of the substituted one is disfavoured by 0.250 eV while the *endo* one is favoured by 0.082 eV. As we have shown, 0.183 eV can be assigned to non-bonded interactions with the substituent. In consequence, about two-thirds of the destabilization of the *exo* transition state is due to steric effects but half the difference between the two activation enthalpies for the substituted radical come from electronic effects. These effects come from two sources. First, the presence of the substituent increases the polarization of the initial olefin[29] and so this effect is now opposed in a stronger way to the worst orientation of the interacting orbitals in the transition state. Second, the substituent stabilizes the incoming α electronic density through the $\pi^*_{CH_3}$ orbital in the *endo* transition state but contributes to the growing of β density in the attacked carbon of the *exo* transition state. We can conclude that both steric and electronic effects co-operate to reverse the regioselectivity of the reaction.

Cyclization of the 2-Methylhex-5-enyl Radical. Effect of a Substituent on the Alkyl Fragment of the Radical and Role of Entropy.—When the methyl substituents are in the alkyl fragment of the radical the cyclization affords the *exo* product as in the unsubstituted radical. Now there are two possible *exo* products (**6**) and (**7**). The stereoselectivity of the reaction depends on the position of the substituents and has been attributed to non-bonded orbital attractions.[34] The alternative explanation based on electrostatic interactions[2a] is unlikely in view of the very small charge densities calculated for the transition states (Table 2).

Neither the activation enthalpies nor the activation entropies distinguish between the *exo* transition states corresponding to (**6**) and (**7**) which we will designate the *exo-trans* and *exo-cis* transition states. These values are 14.7 kcal mol^{-1} and -7.0 cal mol^{-1} K^{-1}, respectively. The activation enthalpy for the *endo* transition state is also 14.7 kcal mol^{-1} and $\Delta S^{\ddagger}$ amounts to -13.0 cal mol^{-1} K^{-1}. As in the unsubstituted case the regioselectivity is due to the more favourable activation entropy for the *exo* transition state but we cannot provide an explanation for the stereoselectivity. There is a small decrease of the activation enthalpy with respect to the unsubstituted case in agreement with the experimental results.[35] The heats of reaction are -19.1, -18.9, and -35.6 kcal mol^{-1} for the *exo-cis*, *exo-trans*, and *endo* cyclizations.

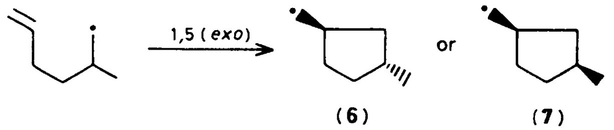

(**6**) (**7**)

The *endo* and *exo-cis* transition states are presented in Figure 3 and the important structural parameters for the reactant, products, and transition states are collected in Table 5. The geometric changes from the initial radical to the transition state are almost identical to those found in the unsubstituted radical as are the results of the energy-partitioning analysis.

The decrease in the activation enthalpy (1.7 kcal mol^{-1}) with respect to the unsubstituted case is worthy of comment. The origin of this effect as revealed from the energy-partitioning analysis lies in the contributions of the C-1–C-2–C-3 fragment. The total contribution of this fragment ($E_{C\text{-}1\text{--}C\text{-}2} + E_{C\text{-}2\text{--}C\text{-}3} + E_{C\text{-}1} + E_{C\text{-}2} + E_{C\text{-}3}$) implies a destabilization of the 2-methylhex-5-enyl radical with respect to the hex-5-enyl radical of 0.923 eV while the destabilization in the transition state amounts only to 0.860 eV. In consequence the activation enthalpy is 0.063 eV smaller in the substituted case. This value

Table 5. Calculated geometries for the reactant, products, and transition states of the 2-methylhex-5-enyl radical cyclization

	Geometry[a,b]
2-Methylhex-5-enyl radical	C-1C-2: 1.475; C-2C-3: 1.538; C-3C-4: 1.516; C-4C-5: 1.491; C-5C-6: 1.327; C-2C-7: 1.517; C-1C-2C-3: 113.6; C-2C-3C-4: 121.7; C-3C-4C-5: 119.1; C-4C-5C-6: 131.9; C-7C-2C-3: 116.2; HC-1C-2: 123.3; H′C-1C-2: 122.8; C-1C-2C-3C-4: 159.7; C-2C-3C-4C-5: 176.4; C-3C-4C-5C-6: 118.7; C-7C-2C-3C-4: 66.1; HC-1C-2C-3: −33.8; H′C-1C-2C-3: 163.1
4-Methylcyclohexyl radical	C-1C-2: 1.540; C-2C-3: 1.539; C-3C-4: 1.521; C-4C-5: 1.477; C-5C-6: 1.476; C-2C-7: 1.515; C-1C-6: 1.519; C-1C-2C-3: 114.1; C-2C-3C-4: 117.7; C-3C-4C-5: 116.9; C-6C-1C-2: 118.2; C-7C-2C-1: 114.62; C-1C-2C-3C-4: 36.8; C-2C-3C-4C-5: −24.7; C-3C-2C-1C-6: −37.2; C-7C-2C-1C-3: 135.1
(*cis*-3-Methylcyclopentyl)methyl radical	C-1C-2: 1.545; C-2C-3: 1.542; C-3C-4: 1.520; C-4C-5: 1.542; C-6C-5: 1.467; C-5C-1: 1.544; C-2C-7: 1.509; C-6C-5C-1: 117.9; C-5C-1C-2: 110.0; C-1C-2C-3: 105.0; C-7C-2H: 104.0; HC-6C-5: 102.6; H′C-6C-5: 122.0; HC-7C-2: 113.0; HC-6C-5H′: 161.0; C-5C-1C-2C-3: 8.4; C-4C-3C-2C-1: 4.7; C-7C-2C-1C-3: 133.2; C-6C-5C-4C-3: 139.8
exo-cis TS	C-1C-2: 1.497; C-2C-3: 1.543; C-3C-4: 1.519; C-4C-5: 1.500; C-5C-6: 1.356; C-2C-7: 1.514; C-1C-5: 2.209; C-1C-2C-6: 108.8; C-2C-3C-4: 116.6; C-3C-4C-5: 116.4; C-4C-5C-6: 129.2; C-7C-2C-3: 116.6; HC-6C-5: 124.9; H′C-6C-5: 123.8; C-1C-5C-6C-4: −109.4; C-2C-3C-4C-5: 20.9; C-3C-4C-5C-6: −134.1; C-7C-2C-3C-4: 124.1; HC-6C-5C-4: 17.9; H′C-6C-5C-4: −170.1
endo TS	C-1C-2: 1.498; C-2C-3: 1.541; C-3C-4: 1.490; C-4C-5: 1.490; C-5C-6: 1.352; C-2C-7: 1.517; C-1C-6: 2.265; C-1C-2C-3: 114.6; C-2C-3C-4: 120.1; C-2C-3C-4: 120.1; C-3C-4C-5: 115.3; C-6C-1C-2: 111.1; C-7C-2C-1: 113.6; HC-6C-5: 122.7; H′C-6C-5: 124.8; C-1C-2C-3C-4: 41.1; C-2C-3C-4C-5: −43.3; C-3C-2C-1C-6: −37.5; C-7C-2C-1C-3: −133.9; HC-6C-5C-4: −171.5; H′C-6C-5C-4: 30.0

[a] Distances in Ångstroms, angles in degrees. [b] See Figure 3 for notation.

Table 6. Standard entropies S^0_{298} and their contributions for the initial radical and transition states of the 2-methylhex-5-enyl and 5-methylhex-5-enyl radical cyclizations. Entropies in cal mol^{-1} K^{-1}

	S°_{total}	S°_{tr}	S°_{rot}	S°_{vib}	$\Delta S^\ddagger$
5-Methylhex-5-enyl radical	100.9	39.6	28.3	32.9	
endo TS	87.9	39.6	27.7	20.6	−12.9
exo TS	91.7	39.6	27.5	24.6	−9.1
2-Methylhex-5-enyl radical	99.8	39.6	28.3	31.8	
endo TS	86.7	39.6	27.7	19.4	−13.0
exo TS	92.8	39.6	27.8	25.4	−7.0

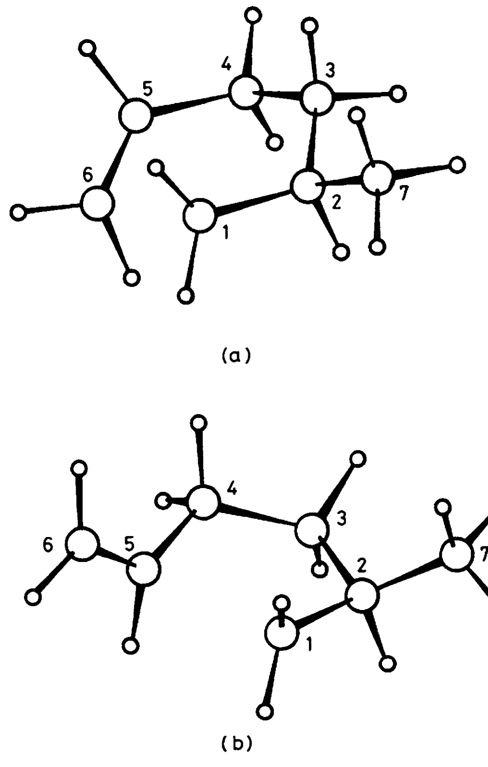

Figure 3. *endo* (a) and *exo-cis* (b) transition states for cyclization of the 2-methylhex-5-enyl radical

is very close to the global value of 0.074 eV and so, as long as the enthalpy is concerned, we can conclude that the increase of the cyclization rate with the methyl substitution at C-2 is due to a smaller destabilization of the C–C bond adjacent to the substituent in the transition states of the substituted radical. These destabilizations can be readily traced back to $\sigma_{C-C}-\pi^*_{CH_3}$ and $\sigma^*_{C-C}-\pi_{CH_3}$ interactions.

It is time to comment on the role of the activation entropy. Within the rigid rotor–harmonic oscillator approximation the total entropy can be partitioned into translational, rotational, and vibrational contributions. The vibrational contribution can be subsequently partitioned in contributions from each normal mode. This gives an easy way to analyse the entropy changes. The calculated values of the entropy and their contributions for the cyclization of the 2-methyl- and 5-methylhex-5-enyl radicals are shown in Table 6.

Let us recall that $\Delta\Delta S^\ddagger$ for the unsubstituted radical was 3.6 cal mol^{-1} K^{-1}. The difference is almost unaltered when the substituent is in the olefinic part of the radical but increases to 6.0 cal mol^{-1} K^{-1} when in the alkyl fragment. In both cases the difference in $\Delta S^\ddagger$ is almost exclusively due to the vibrational contribution. For the unsubstituted and 5-substituted radicals the difference comes from the pseudorotation of the external CH_2 group and three normal modes delocalized all along the ring. In the 2-substituted radical we found the same contributions and that of the pseudorotation of the CH_3 group. The vibrational frequency of this last mode is lower in the *exo* transition state and its contribution to $\Delta\Delta S^\ddagger$ is 1.4 cal mol^{-1}

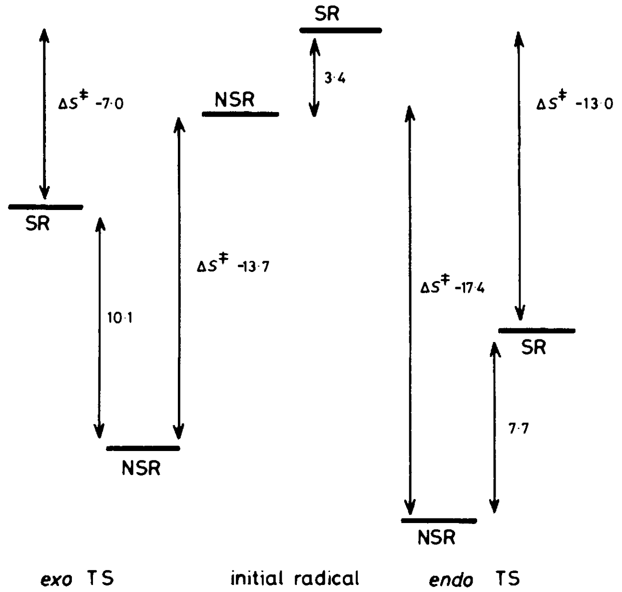

Figure 4. Effect of a methyl substituent on the standard entropies of the initial radical and transition states of the hex-5-enyl radical cyclization. NSR, Non-substituted (hex-5-enyl) radical; SR, substituted (2-methylhex-5-enyl) radical. Entropies in cal mol^{-1} K^{-1}

K^{-1}. The presence of a methyl group in the alkyl fragment of the radical differentiates more between the two transition states because the vibrational frequency of the pseudorotation is lower, its contribution of the entropy is greater, and the small differences between the two transition states become more apparent.

The relation of these results with the Allinger–Zalkow interpretation of the *gem*-dimethyl effect[36] should be pointed out. These authors proposed that the increase in the reaction rate produced by methyl groups in ring-closure reactions leading to substituted cyclohexane molecules was due to a decrease of the activation enthalpy and a more favourable activation entropy. The same explanation was proposed for smaller rings. The entropies of the initial radical and transition states of the unsubstituted hex-5-enyl radical (NSR) and the 5-methylhex-5-enyl radical (SR) are shown in Figure 4. The introduction of the substituent raises by 3.4, 10.1, and 7.7 cal mol^{-1} K^{-1} the entropies of the initial radical, *exo* and *endo* transition state, respectively. If we compare these figures with the variation of standard entropy in cyclohexane, cyclopentane, or alk-1-enes upon introduction of a methyl group,[37] 9.2 cal mol^{-1} K^{-1}, we can conclude that the decrease in the activation entropies with substitution is due to the lesser entropy increase of the initial radical. In consequence, although the origin of the enthalpy contribution is different our discussion of the 5-methylhex-5-enyl cyclization confirms the Allinger–Zalkow interpretation.

In summary, the use of the energy-partitioning analysis within the context of the MINDO/3 method leads to a clear understanding of the origin of the major electronic, steric, and entropic effects competing in the cyclization of the hex-5-enyl radicals. This study complements the previous work by Bischof[10] on the influence of the chain length of the radical on the cyclization. Extension of this type of analysis to alkenylsilyl radicals[38,39] and the comparison with the intermolecular additions would be interesting.

Acknowledgements

We are grateful to Professor S. Olivella for his interest. We thank Professors P. Bischof and S. Olivella for communication of unpublished results.

References

1 J. M. Tedder, *Angew Chem., Int. Ed. Engl.*, 1982, **21**, 401; J. M. Tedder and J. C. Walton, *Tetrahedron*, 1980, **36**, 701; *Adv. Phys. Org. Chem.*, 1978, **16**, 51.
2 For some reviews of intramolecular cyclizations see: (*a*) A. L. J. Beckwith, *Tetrahedron*, 1981, **37**, 3073; (*b*) A. L. J. Beckwith and K. U. Ingold. 'Rearrangements in Ground and Excited States,' ed. P. de Mayo, Academic Press, New York, 1980, vol. 2, p. 161; (*c*) M. Julia, *Pure Appl. Chem.*, 1974, **40**, 553; (*d*) J. M. Surzur, 'Reactive Intermediates,' ed. A. A. Abramovitch, Plenum Press, New York, 1981, vol. 2.
3 S. W. Benson, 'Thermochemical Kinetics,' Wiley, New York, 1976, 2nd edn.
4 R. C. Lamb, P. W. Ayers, and M. K. Toney, *J. Am. Chem. Soc.*, 1963, **85**, 3483.
5 H. Hart and D. Wyman, *J. Am. Chem. Soc.*, 1959, **81**, 4891.
6 C. Walling and A. Gioffari, *J. Am. Chem. Soc.*, 1972, **94**, 6059.
7 A. L. J. Beckwith and G. Moad, *J. Chem. Soc., Chem. Commun.*, 1974, 472.
8 B. Capon and C. W. Rees, *Annu. Rep. Chem. Soc.*, 1964, **61**, 221.
9 R. D. Rieke and N. A. Moore, *J. Org. Chem.*, 1972, **37**, 413.
10 P. Bischof, *Helv. Chim. Acta*, 1980, **63**, 1434; *Tetrahedron Lett.*, 1979, 1291.
11 M. Julia, C. Descoins, M. Baillarge, B. Jacquet, D. Uguen, and F. A. Graeger, *Tetrahedron*, 1975, **31**, 1737.
12 A. L. J. Beckwith and T. Lawrence, *J. Chem. Soc., Perkin Trans. 2*, 1979, 1535.
13 A. L. J. Beckwith, *Chem. Soc. Special Publ.*, 1970, **24**, 239.
14 A. Effio, D. Griller, K. U. Ingold, A. L. J. Beckwith, and A. K. Serelis, *J. Am. Chem. Soc.*, 1980, **102**, 1734.
15 A. L. J. Beckwith, G. E. Gream, and D. L. Struble, *Aust. J. Chem.*, 1972, **25**, 1081.
16 D. L. Struble, A. L. J. Beckwith, and G. E. Gream, *Tetrahedron Lett.*, 1968, 3701.
17 A. L. J. Beckwith, I. Blair, and G. Phillipou, *J. Am. Chem. Soc.*, 1966, **88**, 5361.
18 A. L. J. Beckwith and W. B. Gara, *J. Chem. Soc., Perkin Trans. 2*, 1975, 593.
19 A. L. J. Beckwith and G. F. Meijs, *J. Chem. Soc., Chem. Commun.*, 1981, 136.
20 E. Canadell, J. M. Poblet, and S. Olivella, *J. Phys. Chem.*, 1983, **87**, 424; S. Olivella, E. Canadell, and J. M. Poblet, *J. Org. Chem.*, 1983, **48**, 4696.
21 J. M. Poblet, E. Canadell, and T. Sordo, *Can. J. Chem.*, 1983, **61**, 2068.
22 M. J. S. Dewar and S. Olivella, *J. Am. Chem. Soc.*, 1978, **100**, 5290.
23 M. J. S. Dewar and S. Olivella, *J. Am. Chem. Soc.*, 1979, **101**, 4958.
24 H. Fischer and H. Kollmar, *Theor. Chim. Acta*, 1970, **16**, 163; M. J. S. Dewar and D. H. Lo, *J. Am. Chem. Soc.*, 1971, **93**, 7201; L. M. Molino and E. Canadell, *Theor. Chim. Acta*, 1981, **60**, 299.
25 R. C. Bingham, M. J. S. Dewar, and D. H. Lo, *J. Am. Chem. Soc.*, 1975, **97**, 1286.
26 W. C. Davidon, Research and Development Report 5990, Argonne National Laboratory, 1959; R. Fletcher and M. J. D. Powell, *Comput. J.*, 1963, **6**, 163.
27 J. W. McIver and A. Komornicki, *J. Am. Chem. Soc.*, 1972, **94**, 2625.
28 M. J. S. Dewar and G. P. Ford, *J. Am. Chem. Soc.*, 1977, **99**, 7822.
29 I. Lee, *Tetrahedron*, 1983, **39**, 2409; I. Lee, B.-S. Lee, C. H. Song, and C. K. Kim, *Bull. Korean Chem. Soc.*, 1983, **4**, 84.
30 H. Fujimoto, S. Yamabe, T. Minato, and K. Fukui, *J. Am. Chem. Soc.*, 1972, **94**, 9205.
31 L. Libit and R. Hoffmann, *J. Am. Chem. Soc.*, 1974, **96**, 1370.
32 R. C. Bingham, M. J. S. Dewar, and D. H. Lo, *J. Am. Chem. Soc.*, 1975, **97**, 1294.
33 A. L. J. Beckwith, I. A. Blair, and G. Phillipou, *Tetrahedron Lett.*, 1974, 2251.
34 A. L. J. Beckwith, I. Blair, and G. Phillipou, *J. Am. Chem. Soc.*, 1974, **96**, 1613.
35 A. L. J. Beckwith, T. Lawrence, and A. K. Serelis, *J. Chem. Soc., Chem. Commun.*, 1980, 484.
36 N. Allinger and V. Zalkow, *J. Org. Chem.*, 1960, **25**, 701.

37 'Handbook of Chemistry and Physics,' CRC Press, Palm Beach, 1978, 58th edn.
38 C. Chatgilialoglu, H. Woynar, K. U. Ingold, and A. G. Davies, *J. Chem. Soc., Perkin Trans. 2*, 1983, 555.
39 T. Barton and A. Revis, *J. Am. Chem. Soc.*, 1984, **106**, 3802.

Received 18*th September* 1984; *Paper* 4/1617